Journal of Food Process Engineering

WILEY

Journal of Food Process Engineering

ORIGINAL ARTICLE OPEN ACCESS

Real-Time Monitoring of Refrigerated Storage Using a Wireless Sensor Network: Development and Validation of the UMITEMP System

Murilo Santos Freire[1] | Daniel dos Santos Costa[1] | Alisson Pereira dos Santos[2] | Sérgio Tonetto de Freitas[3] | Magno do Nascimento Amorim[4] | Silvia Helena Nogueira Turco[1]

[1]Graduate Program in Agricultural Engineering, Universidade Federal do Vale do São Francisco (Univasf), Juazeiro, Bahia, Brazil | [2]Department of Computer Engineering, Universidade Federal do Vale do São Francisco (Univasf), Juazeiro, Bahia, Brazil | [3]Postharvest Physiology and Technology Laboratory, Empresa Brasileira de Pesquisa Agropecuária (Embrapa Semiárido), Petrolina, Pernambuco, Brazil | [4]Department of Agricultural Engineering, Instituto Federal Goiano (IFGoiano), Urutaí, Goiás, Brazil

Correspondence: Magno do Nascimento Amorim (magno_amorim27@hotmail.com)

Received: 16 November 2025 | **Revised:** 22 April 2026 | **Accepted:** 8 May 2026

Keywords: cold room storage | real-time monitoring | web applications | wireless sensor network

ABSTRACT

The objective of this study was to develop and validate UMITEMP, an intuitive system for real-time monitoring of air temperature (Ta) and relative humidity (RH) in cold rooms for table grape storage. The system integrates hardware and software with wireless radio-frequency communication and a web-based interface. A wireless sensor network (WSN) was distributed within the cold room, collecting data every minute and displaying it in interactive charts and maps. Individual calibration of capacitive humidity sensors was required to ensure accuracy. WSN signal quality was unaffected by wall insulation or sensor distance. During the experimental period, RH ranged from 71% to 100%, averaging 85%, below the recommended level for seedless grape storage. The average Ta was 0.4°C, slightly above the ideal range, with maxima of 5.4°C and minima of −1.9°C. Internal spatial variability was observed, with lower Ta and RH variance than in the adjacent corridor, which was more influenced by external conditions and showed temperature increases during weekdays. Results demonstrate that UMITEMP is an effective tool for continuous real-time monitoring of cold rooms, supporting proper management of fresh fruit storage, such as table grapes.

1 | Introduction

Viticulture is a competitive agricultural sector, marked by shifts in consumption patterns and increasing demand for fresh foods with assured nutritional, sanitary, and sensory quality (Lazzarotto and Fioravanço 2012). Among nonclimacteric fruits, table grapes are among the most sensitive to storage conditions, being highly vulnerable to variations in temperature and relative humidity (RH). The main factors affecting their shelf life include deterioration caused by *Botrytis cinerea*, as well as peduncle and berry dehydration (Pereira et al. 2018), both directly linked to the need for precise control of temperature and RH in storage facilities (Amorim et al. 2020; Miranda et al. 2025).

Refrigerated storage is widely used to slow metabolic activity and preserve postharvest quality (Amorim et al. 2022; Santos et al. 2025). Ideal conditions for table grapes range from −1°C to 0°C for air temperature (Ta) and from 90% to 95% for RH (Durner 2013). Values outside these ranges can increase the incidence of decay and dehydration, as well as cause freezing damage at temperatures ≤ −3°C (Gross et al. 2016). Temperature fluctuations during storage represent an additional problem, as they can lead to condensation on the fruit, favoring microbial growth and reducing shelf life. Such changes are often detected only at advanced stages, when visible signs of deterioration are already present, highlighting the need for efficient systems to monitor Ta and RH (Badia-Melis, Mishra, et al. 2015).

In commercial practice, environmental monitoring is still largely based on data loggers and a limited number of sensors, which often lack real-time accessibility and require manual data retrieval, limiting continuous decision-making (Khumalo et al. 2023; Habib et al. 2024). Furthermore, temperature deviations throughout the cold chain are recognized as a major factor contributing to food loss, quality degradation, and economic impacts, reinforcing the importance of continuous monitoring (Canatan et al. 2025). As a result, these approaches may not adequately represent the spatial and temporal variability inside cold rooms, allowing localized deviations from recommended storage conditions to remain undetected, particularly during routine operations such as loading, unloading, and door opening.

Growing concern over food safety and the reduction of post-harvest losses has driven the adoption of automated supply chains with continuous monitoring systems. Tracking environmental conditions throughout the cold chain is essential to prevent failures in storage, transportation, and marketing, ensuring compliance with quality standards and consumer protection (Badia-Melis et al. 2018). In this context, wireless sensor network (WSN) and Internet of Things (IoT)-based technologies have gained prominence in agricultural monitoring and cold chain management (Karimi et al. 2018; Mohammed et al. 2022; Garrido-López et al. 2024). Radiofrequency (RF)-based solutions show promise for cold chain management, as they reduce labor costs, increase efficiency, and improve the traceability of perishable products (Kumari et al. 2015). However, smart systems generate large volumes of high-velocity data, requiring tools that facilitate intuitive interpretation and visualization to support decision-making (Kamilaris et al. 2017).

Nevertheless, many monitoring solutions currently available are primarily focused on data logging or general environmental supervision, with limited emphasis on sensor-level calibration, spatial interpretation of microclimatic variability, and integrated real-time visualization tailored to decision-making in refrigerated fruit storage. In addition, limitations related to sensor accuracy and calibration remain a critical issue, particularly for low-cost sensing systems, where calibration procedures are essential to ensure reliable measurements (Rivero et al. 2023; Zhang et al. 2024). Moreover, recent studies highlight that the use of multiple sensors combined with appropriate data interpretation strategies is essential to detect localized critical points and reduce false alarms in cold chain monitoring systems (Whitaker and Dawson 2025).

In addition, although commercial monitoring technologies are available, studies demonstrating the development and validation of integrated systems under real cold-room operating conditions remain relevant, particularly when they combine calibrated sensing, robust wireless communication, and tools for interpreting spatial and temporal variability. For highly perishable products such as table grapes, these aspects are essential not only for recording average environmental conditions, but also for identifying localized fluctuations that may compromise product quality, given the well-documented heterogeneity of storage conditions and shelf life within the same batch (Oliveira et al. 2020; Fabri et al. 2025).

Therefore, the contribution of this study lies not merely in the use of wireless sensing, but in the integration and validation of a monitoring system capable of (i) acquiring calibrated Ta and RH data in real time, (ii) maintaining stable wireless communication in an insulated refrigerated environment, and (iii) providing temporal and spatial analyzes through a web-based interface to support storage management. This approach aims to bridge the gap between environmental monitoring and decision-oriented tools in cold chain management. The objective of this study was to develop and validate the UMITEMP system, a real-time monitoring system for air temperature and relative humidity in cold rooms used for table grape storage.

2 | Materials and Methods

The UMITEMP system was designed to monitor air temperature and relative humidity in table grape cold rooms. This tool collects data via sensors installed inside the cold rooms, transmitting them to a microcomputer located on-site, and making the information available on a web page (umitemp.tk).

For acquiring the physical variables (Ta and RH), a self-organizing WSN was used, which collects data every minute. Data storage and processing were performed using a relational database management system (RDBMS) and a web application, responsible for generating dynamic charts and maps of the variables analyzed in the cold room. Figure 1 provides an overview of the monitoring system.

2.1 | Real-Time Monitoring System

The developed system consisted of a WSN designed for continuous monitoring of environmental conditions in cold storage chambers. Considering the harsh environmental conditions—characterized by near-saturation relative humidity that can cause oxidation, short circuits, and RF signal interference—all electronic components were properly sealed and subjected to preliminary transmission tests to ensure system robustness.

The network was composed of 12 slave units (SUs) distributed within the cold chamber, each equipped with temperature and humidity sensors, a radiofrequency module, and a microcontroller board. An additional SU was placed in the external corridor for supplementary monitoring of environmental conditions. The master unit (MU), equipped with a radiofrequency module and a serial interface, received data from the SUs and transmitted them to a central base (CB).

The CB processed and stored the data in a RDBMS, making the information available through a web interface for remote monitoring. Communication between nodes followed a mesh topology, in which each SU could act as a relay, ensuring network self-organization and fault tolerance. This approach guaranteed continuous operation even in the event of individual node failures, offering greater reliability compared to conventional hierarchical networks. This implementation enabled real-time monitoring of environmental variables, with adaptability to the specific conditions of commercial cold storage facilities. The firmware embedded in the WSN hardware is shown in Figure 2.

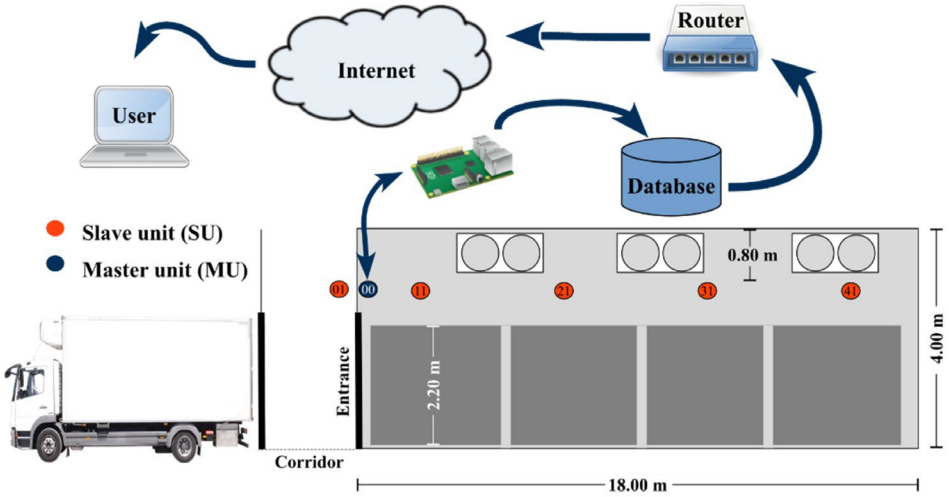

FIGURE 1 | Conceptual architecture of the UMITEMP system for grape cold storage rooms. Slave unit (SU), a microcontrolled device used to measure Ta and RH. Master unit (MU), a microcontrolled device used to collect and transfer all SU data to the database.

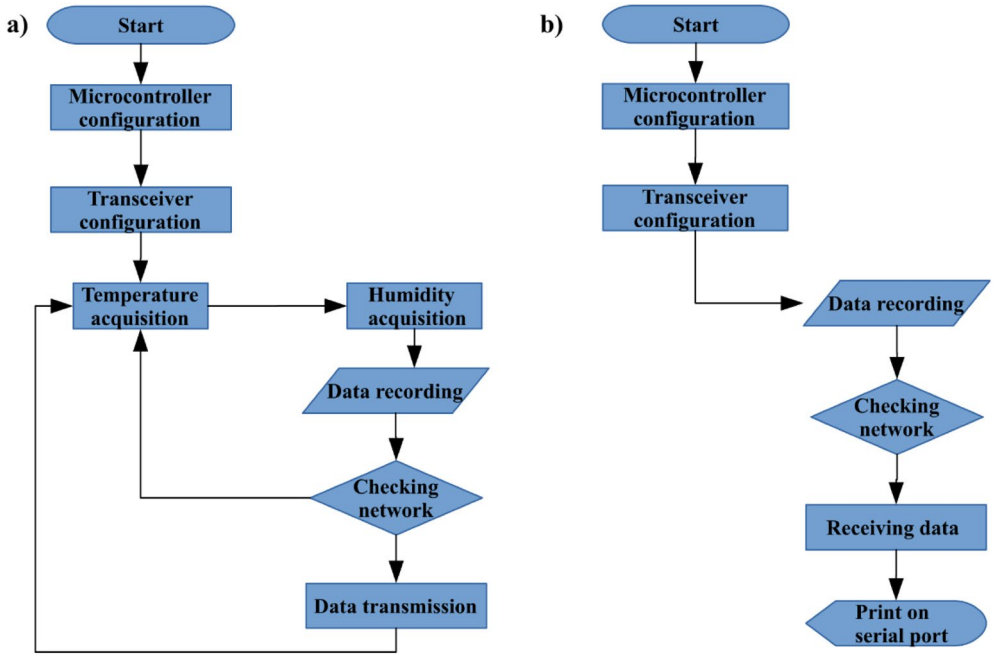

FIGURE 2 | Flowchart of the firmware shipped in SU (a) and MU (b).

2.2 | Slave Units (SU)

The SU were designed with three main components: sensing elements, a radio frequency module, and a microcontroller, complemented by a microSD card slot that enabled their operation as data loggers, Figure 3 shows the SU block diagram. The core of the system was based on the ATmega328P microcontroller (Atmel Corporation, California, USA), which managed all processes through its 10-bit analog-to-digital (A/D) converters and an internal 1.1 V reference voltage. This configuration allowed the acquisition of low-voltage signals without the need for additional signal conditioning circuits. Communication between components was established via the Serial Peripheral Interface (SPI) protocol.

For relative humidity measurement, the capacitive HIH 4000-001 sensor (Honeywell International Inc., Minnesota, USA) was selected due to its integrated signal conditioning, robustness in refrigerated environments, and measurement range of 0%–100% RH with an accuracy of ±3.5% RH. This sensor has a response time of approximately 5 s, operates with a power supply of 4–5.8 V, and outputs the measurement in voltage. To ensure higher accuracy, each sensor was individually calibrated following the methodology validated by (Nair et al. 2015).

Air temperature was measured using the LM35DZ integrated circuit sensor (Texas Instruments Inc., Texas, USA), which provides a linear output, ±0.5°C accuracy, and a wide operational range from −55°C to 150°C, with a response time of around 60 s

in still air. This sensor can be powered from 4 to 30 V and also outputs the measurement in voltage, without requiring external calibration. For measurements at subzero temperatures, a circuit employing a 1N4007 diode was implemented to create a voltage offset, eliminating the need for a negative power supply.

The communication module employed the nRF24L01 transceiver (Nordic Semiconductor, Oslo, Norway), operating in the 2.4 GHz band with adjustable output power between −20 and 0 dBm. This component offered several advantages: (1) configurable data rate between 250 and 2000 Kbps, with lower rates providing higher sensitivity; (2) 126 communication channels with a range of up to 100 m; (3) packet size limited to 32 bytes, reducing losses during transmission; and (4) low energy consumption due to fast switching between transmit and receive modes.

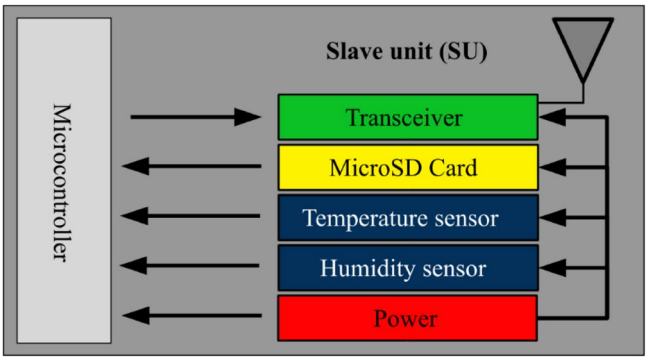

FIGURE 3 | SU hardware block diagram.

2.3 | Master Unit (MU) and Central Base (CB)

The Master Unit (MU) shared the same basic architecture as the SUs, using the same ATmega328P microcontroller and nRF24L01 transceiver, but in a simplified configuration. Unlike the SUs, the MU incorporated a Light Dependent Resistor (LDR) sensor for monitoring ambient light levels, while the SUs were dedicated exclusively to air temperature and relative humidity measurements. The wireless network configuration was optimized to operate at a low data rate (250 Kbps), a strategy that increased the effective communication range between the MU and the most distant SU. Figure 4 shows a block diagram of the MU.

The interface between the MU and the CB was implemented through serial communication, enabling a continuous data flow for storage and processing. The CB, based on a Raspberry Pi 3 platform (Raspberry Pi Foundation, Cambridge, UK), performed three main functions: (1) storing the collected data in a relational database, (2) processing the information to generate performance indicators, and (3) functioning as a gateway to make the data available through a web-based application accessible via the Internet.

2.4 | Web-Based Application

The UMITEMP system incorporated a web application developed as a graphical interface for accessing and analyzing the collected data. The architecture of the solution was based on an SQL relational database that automatically received and organized the measurements transmitted by the MU (Figure 5).

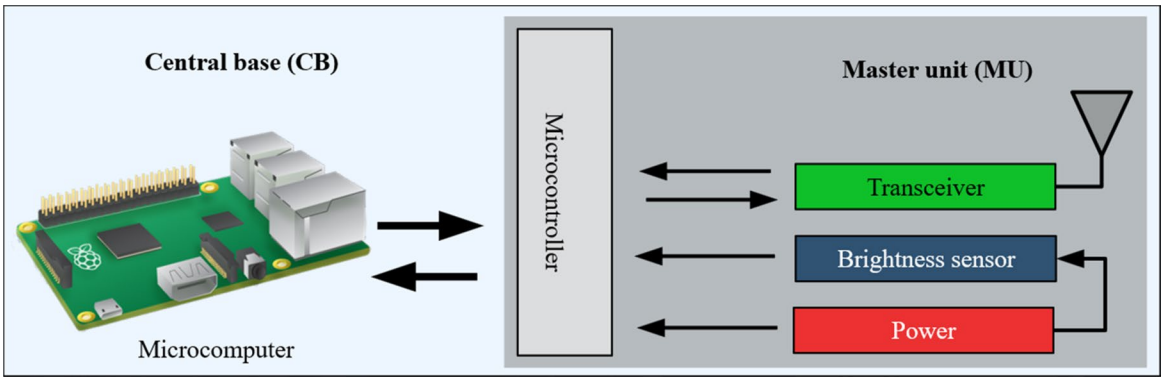

FIGURE 4 | Block diagram of the master unit (MU) and communication with the central base (CB).

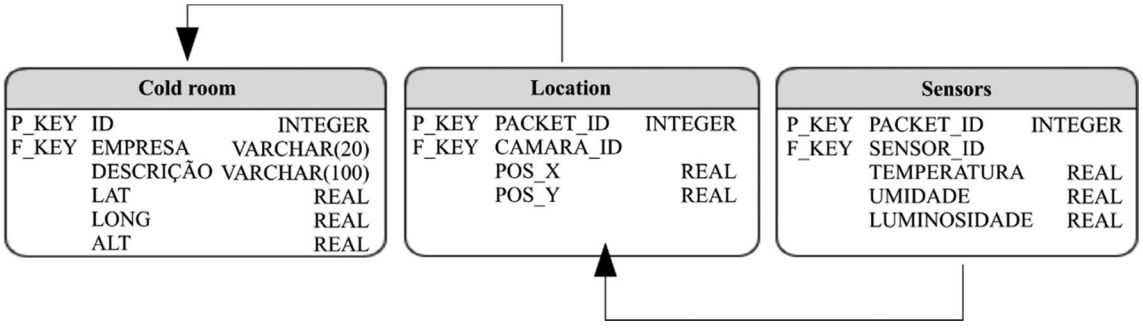

FIGURE 5 | Database model used in the UMITEMP system.

Data processing was performed in real time, enabling immediate availability through the web platform.

Figure 6 shows the use case diagram describing the sequences of interactions (UC) that users can have with the UMITEMP system.

User interaction with the system occurred through eight main use cases, each providing a different analytical perspective:

- *Cold Room Overview (UC01):* Presents aggregated statistics (maximum, minimum, and mean values) for Ta and RH over the selected time period.
- *Slave Unit Overview (UC02):* Provides individual statistical analysis for each SU, enabling sensor-specific evaluation.
- *Temporal Analysis (UC03):* Generates dynamic plots of Ta and RH variation over time, with interactive zoom for the desired period.
- *Psychrometric Analysis (UC04):* Displays the psychrometric chart constructed from the data collected within the specified interval.
- *Spatial Analyzes (UC05–UC06):* Produces thermal and humidity maps representing the spatial distribution of variables inside the cold room.
- *Network Performance (UC07):* Technical report containing signal quality metrics for each SU, with filtering by period.
- *Project Information (UC08):* Reference documentation regarding the research supporting the development of the system.

The interface was designed for maximum flexibility, allowing users to freely select analysis time intervals across all visualizations. Data representation included both tabular formats for precise value inspection and dynamic visualizations for pattern and trend identification. The UMITEMP system provides real-time visualization through its web-based interface, including temporal graphs of air temperature and relative humidity, selectable time resolutions (e.g., minute or hourly intervals), and psychrometric charts based on the recorded data. However, the spatial interpolation maps and derived statistical analyzes presented in this study were generated through postprocessing of the collected data using specialized geostatistical software, for scientific analysis purposes.

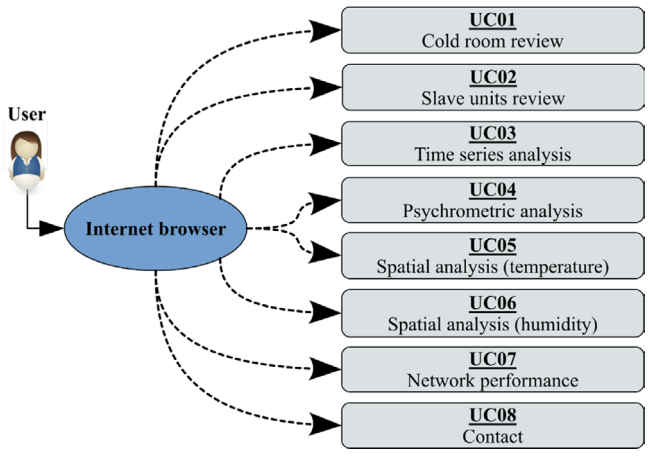

FIGURE 6 | Use case diagram of the UMITEMP system web application.

2.5 | Humidity Sensor Calibration

The calibration of the humidity sensors was performed using the saturated salt solution method, a recognized secondary standard (WMO 2008), which establishes hygroscopic equilibrium between the saline solution and the surrounding air in a controlled environment. All 13 sensor units used in the study, including those installed in the cold chamber and the access corridor, were subjected to this calibration procedure. The calibration procedure was conducted under laboratory ambient conditions (approximately 25°C ± 2°C), consistent with the reference conditions reported for saturated salt solutions (Greenspan 1977). Six saturated saline solutions (30 mL each) were prepared according to Greenspan (Greenspan 1977): potassium hydroxide (7.38% RH), magnesium chloride (32.44% RH), potassium carbonate (43.17% RH), sodium chloride (75.09% RH), potassium chloride (83.62% RH), and potassium sulfate (97.00% RH), covering a relative humidity range from 7.38% to 97.00%. The sensors were placed inside hermetically sealed 50 mL containers, where they remained for 60 min to stabilize prior to data acquisition, which was performed at 1-min intervals over a 90-min period for each solution. During this process, the solution surface area exceeded that of the sensor, and the air volume was minimized to optimize equilibrium conditions.

The collected data were processed to generate individual calibration equations, whose statistical validation included the calculation of correlation coefficients (R) and determination coefficients (R^2), analysis of variance, and comparison with the manufacturer's model using the Mean Squared Error (MSE—Equation 1), and Mean Absolute Error (MAE—Equation 2). This approach follows established protocols to ensure the accuracy of humidity measurements, with MSE emphasizing larger deviations and MAE providing an intuitive measure of average error.

$$\mathrm{MSE} = \frac{1}{N}\sqrt{\sum \left(X_{\mathrm{ME}} - X_{\mathrm{CE}}\right)^2} \tag{1}$$

$$\mathrm{MAE} = \frac{\sum \left|X_{\mathrm{ME}} - X_{\mathrm{CE}}\right|}{N} \tag{2}$$

where MSE = mean squared error, % RH; MAE = mean absolute error, % RH; X_{ME} = manufacturer's humidity equation, % RH; X_{CE} = humidity from the calibration equation, % RH; N = number of samples.

2.6 | Experimental Evaluation in a Cold Room

The system was tested in an experimental cold room measuring 2 × 2 × 2 m, constructed with 10 cm polystyrene walls coated with a double layer of 10 mm zinc plates, and equipped with a refrigeration system based on evaporators. The refrigeration system consisted of a conventional air-cooling unit equipped with finned evaporator coils and axial fans to promote air circulation within the chamber. To simulate the actual storage conditions for table grapes, which require Ta between −1°C and 0°C and RH between 90%–95%, the following protocol was implemented: initially, the evaporators were switched off, and the cold room door was kept

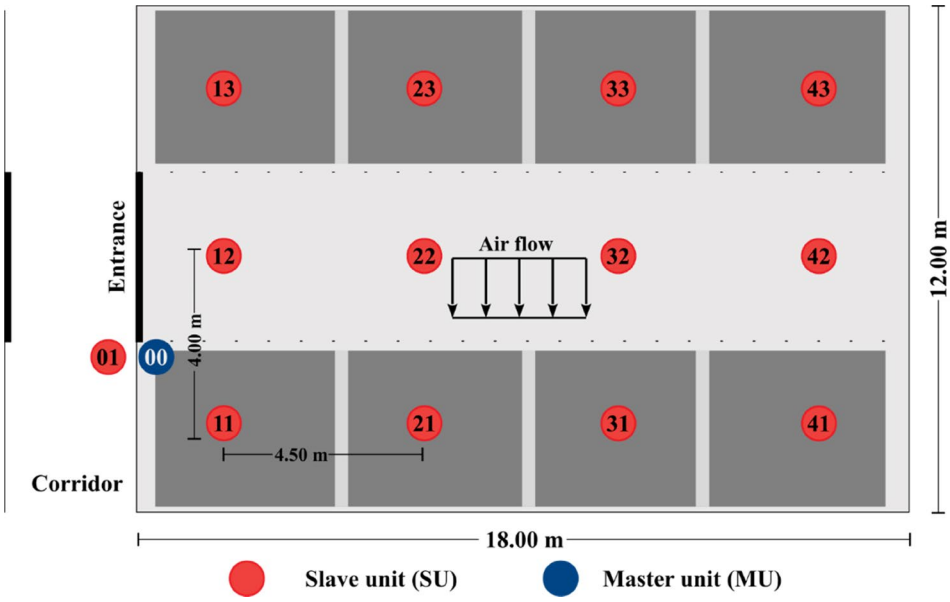

FIGURE 7 | Spatial distribution of the UMITEMP system's sensors in the cold room and the access corridor to the cold room.

open for 10 min to equalize the internal Ta with the external ambient temperature. After closing the room, the condenser temperature was set to −10°C. After 1 h of operation, the cold room door was opened for approximately 10 min to simulate the inflow of warm air during loading and unloading operations, thereby exposing the sensors to abrupt thermal and humidity variations typical of such processes. After closing, the system was allowed to stabilize for 30 min before the next opening event. This open/close cycle was repeated twice, subjecting the sensors to dynamic conditions representative of commercial cold room operations.

A total of 12 sensor units were used in the experimental cold room evaluation, corresponding to the sensors installed inside the chamber. Prior to system assembly, the sensors were calibrated using a CS215 thermo-hygrometer as a reference. Due to the reduced dimensions of the chamber, the sensors were installed at an approximate height of 1.0 m from the floor, using a support structure (Campbell enclosure), allowing the measurement of air conditions representative of the internal environment.

2.7 | Implementation of the UMITEMP System in Real Operating Conditions

Following calibration and validation procedures in a controlled environment, the UMITEMP system was installed in a commercial cold room for export-grade table grapes, located in Petrolina (Pernambuco, Brazil; 9.33851°S, 40.46837°W). The facility measured 12×18×4 m, with a 2×3 m door, insulated with 10 cm polystyrene panels coated with 10 mm zinc plates, and equipped with three evaporators operating between −1°C and 1°C. The cold room was equipped with a refrigeration system based on forced air circulation, using ceiling-mounted cooling units to maintain the desired temperature conditions. The facility was also equipped with a humidification system based on sprinklers, used to assist in maintaining relative humidity levels inside the cold room. The sensor network was deployed in a regular grid of 4.0×4.5 m, totaling 12 SUs strategically positioned inside the cold room (Figure 7). The sensors were installed above the grape pallets, at an approximate distance of 1.5 m below the ceiling of the cold room. Considering that the pallets can reach up to approximately 2.20 m in height, this positioning ensured that the sensors were located just above the upper layer of the stored product, allowing the monitoring of air conditions representative of the microclimate surrounding the grapes. The positioning of the sensors considered the spatial distribution of the stored grapes, which were arranged in pallets, ensuring that the measurements reflected the microclimatic conditions surrounding the product rather than localized airflow near the cooling system. The MU was installed above the entrance door, while an additional SU was placed in the access corridor for supplementary monitoring. The corridor environment was not continuously climatized; however, it was occasionally subjected to temperature control depending on operational conditions. These intermittent cooling periods resulted in variations in temperature and relative humidity, which were captured by the monitoring system. The system core, consisting of a Raspberry Pi 3 serving as the central base, was mounted in the upper section of the cold room, where it performed data processing and hosted the web application that provided, in real time: (i) temporal analyzes of Ta and RH, (ii) dynamic psychrometric charts, and (iii) spatial distribution maps of the monitored variables.

2.8 | Data Transmission Analysis

To evaluate the quality of data transmission in the WSN, two primary traffic indices were employed: the Packet Delivery Rate (PDR) and the Packet Loss Rate (PLR). The PDR, calculated according to Equation (3), represents the ratio between received packets and transmitted packets, serving as an indicator of routing reliability. Complementarily, the PLR (Equation 4) quantifies the percentage of losses during transmission, obtained from the difference between the total number of transmitted packets and those successfully received. Data were collected continuously over a 24-h period, allowing for the assessment of both

overall network performance and the individual behavior of each Slave Unit (SU).

$$\mathrm{PDR} = \frac{\sum P_r}{\sum P_d} \times 100 \tag{3}$$

$$\mathrm{PLR} = \frac{\left(\sum P_d - \sum P_r\right)}{\sum P_d} \times 100 \tag{4}$$

where PDR = packet delivery rate; PLR = packet loss rate; Pr = total number of received packets; Pd = total number of transmitted packets.

Data processing was carried out using the Pandas (v0.22.0) and SciPy (v1.13.0) packages in a Python environment, both well-suited for handling large datasets. Additionally, descriptive statistical analysis was applied to characterize the spatial distribution of data both inside the cold storage room and in the access corridor, ensuring a comprehensive system evaluation.

2.9 | Comparative Analysis Between Environments

To evaluate the relationship between environmental conditions in the cold room and the access corridor, the Pearson correlation coefficient (R) and covariance (COV) were calculated. The correlation coefficient was determined according to Equation (5), and the covariance was calculated using Equation (6):

$$R = \frac{\sum \left(X_i - \overline{X}\right)\left(Y_i - \overline{Y}\right)}{\sqrt{\sum \left(X_i - \overline{X}\right)^2 \sum \left(Y_i - \overline{Y}\right)^2}} \tag{5}$$

$$\mathrm{COV} = \frac{\sum \left(X_i - \overline{X}\right)\left(Y_i - \overline{Y}\right)}{N} \tag{6}$$

where X_i and Y_i represent the observed values in the cold room and corridor, respectively, and $\grave{X}$ and $\grave{Y}$ are their mean values.

2.10 | Psychrometric Analysis

The psychrometric properties of the air were determined according to the parameters established by (ASAE 1998), which allow for the calculation of all psychrometric variables from two known independent properties, considering an air–water vapor mixture and the local atmospheric pressure. For analyzing the data collected inside and outside the monitored facility, the humidity ratio (H) of the air was calculated using Equations (7) through (10), enabling the construction of psychrometric curves representative of the experimental conditions evaluated.

$$\ln P_s = 31.9602 - \frac{6270.3605}{T_a} - 0.46057 \ln T_a \qquad 255.38 \le T_a \le 273.16 \tag{7}$$

$$\ln\left(P_s / R\right) = \frac{\mathrm{A} + \mathrm{B}T_a + \mathrm{C}{T_a}^2 + \mathrm{D}{T_a}^3 + \mathrm{E}{T_a}^4}{\mathrm{FG} - \mathrm{G}{T_a}^2} \tag{8}$$

$$P_v = P_s \frac{\mathrm{RH}}{100} \tag{9}$$

$$H = \frac{0.6219 P_v}{P_{\mathrm{atm}} - P_v} \tag{10}$$

where T_a = air temperature (K); R = 22,105,649.25; A = −27,405.526; B = 97.5413; C = −0.146244; D = 0.12558×10^{-3}; E = -0.48502×10^{-7}; F = 4.34903; G = 0.39381×10^{-2}; H = humidity ratio (kg water vapor kg^{-1} dry air); RH = relative humidity (%); P_v = water vapor pressure (Pa); P_s = saturation pressure (Pa); P_{atm} = atmospheric pressure (Pa).

The psychrometric charts were constructed using temperature and relative humidity data recorded at 1-min intervals. For the cold room, the values used in the analysis correspond to the average of all sensor units at each time step, whereas the corridor data were obtained from the sensor installed in that location. This approach ensures the representation of temporal variability under real operating conditions.

2.11 | Spatial Analysis of Microclimatic Variables

To characterize the spatial distribution of Ta and RH in the cold storage chamber, the Inverse Distance Weighting (IDW) interpolation method was adopted. This deterministic approach, implemented in SAGA GIS (version 2.3.2), was selected based on: (i) the limited number of sensors available, (ii) the need for computational efficiency, and (iii) the objective of highlighting spatial gradients of the monitored variables. Although it offers lower accuracy than geostatistical methods, IDW has been reported as an adequate approach for representing spatial patterns in comparative analyzes, particularly when the objective is to highlight general gradients rather than perform high-precision spatial estimation (Badia-Melis, Ruiz-Garcia, et al. 2015; Ibrahim and Nasser 2015).

The microclimatic variation between the corridor and the interior of the cold room was quantified by calculating the normalized difference, adapted from (Badia-Melis, Ruiz-Garcia, et al. 2015). Equation (11) relates the measured parameters to the refrigeration system's setpoint values, while Equation (12) analyzes the relative variance between environments, allowing for a systematic evaluation of fluctuations in air properties inside the cold chamber. The normalized difference was calculated for each sensor position individually, allowing the spatial variability within the cold room to be properly represented.

$$\text{Normalized difference} = \frac{P_{\text{cold room}} - P_{\text{setpoint}}}{P_{\text{corridor}} - P_{\text{setpoint}}} \tag{11}$$

$$\text{Variance} = \frac{P_{\text{cold room}}}{P_{\text{corridor}}} \tag{12}$$

where P = analyzed parameters: T_a (°C) and RH (%).

3 | Results and Discussion

3.1 | Performance of Humidity Sensors

The calibration results of the capacitive sensors, presented in Table 1, demonstrated excellent performance according to the statistical parameters analyzed. Only the sensors installed inside the cold chamber are presented in this table, as they were used for calibration performance evaluation, while the corridor sensor was used exclusively for comparative environmental analysis. The correlation (R) and determination coefficients ($R^2 > 0.99$) for all sensors indicated a strong linear relationship between the analog responses and the reference values of saline solutions. The statistical significance of the coefficients was confirmed through analysis of variance (F-test, $p < 0.01$), validating the effectiveness of the adopted calibration method.

However, the comparison between the values obtained using the manufacturer's equation and those derived from the calibration models revealed significant discrepancies, particularly for sensors 9 (MSE = 7.10% RH) and 10 (MSE = 11.29% RH). These findings corroborate previous studies: (Mayer et al. 2005) reported variations of 1.2%–12% RH in similar sensors, while (Nair et al. 2015) highlighted the progressive degradation of accuracy in such devices. Our results reinforce the critical need for prior and periodic individual calibration of these sensors, as demonstrated by the MAE and MSE values, which quantify the improvements achieved through the applied calibration procedure.

3.2 | Performance of the UMITEMP System in the Experimental Cold Room

The results showed significant differences between RH measurements obtained with individualized calibration equations and those provided by the manufacturer (Figure 8a). Curves based on the manufacturer's equation tended to overestimate RH values, frequently exceeding 100% RH, due to electrical voltages above the limits specified in the datasheet. This finding reinforces the importance of periodic calibration for electrical RH sensors, particularly for metal oxide types (Webster and Eren 2018) and polymer types (Korotcenkov 2018), which undergo degradation in humid environments.

Figure 8b illustrates the temporal dynamics of Ta and RH during simulated cold room door opening/closing cycles, reproducing real operating conditions during pallet loading and unloading of grapes. A characteristic inverse relationship between Ta and RH was observed: as temperature decreased, a corresponding increase in RH occurred. The system recorded Ta variations between −4.85°C and 28.64°C, and RH variations between 43.72% and 99.60%, demonstrating the robustness of the selected sensors for operating under extreme conditions typical of commercial cold rooms.

Door-opening events allowed for the characterization of humidity peaks resulting from the mixing of cooled internal air with external ambient air. These data validate the UMITEMP system's capability to monitor the microclimatic fluctuations typical of logistical operations in refrigerated storage units. Beyond system validation, these results are particularly relevant for table grape storage, as rapid temperature and humidity fluctuations are directly associated with condensation processes, which may accelerate fungal development and reduce shelf life. Therefore, the ability of the system to detect such short-term variations provides valuable information for improving operational practices in cold rooms, especially during loading and unloading events. Furthermore, continuous monitoring of dynamic environmental conditions is essential to support decision-making and reduce postharvest losses in cold chain systems (Chaudhuri et al. 2018; Oliveira et al. 2020).

TABLE 1 | Individual calibration of humidity sensors.

Humidity sensor	Calibration curve	R	R^2	MSE	MAE
Sensor 1	0.031× + 0.970	1.000	1.000	3.64	3.53
Sensor 2	0.030× + 0.949	1.000	0.999	2.38	1.98
Sensor 3	0.030× + 0.951	1.000	0.999	2.26	1.74
Sensor 4	0.030× + 0.987	1.000	1.000	2.93	2.45
Sensor 5	0.030× + 1.014	1.000	1.000	4.03	3.83
Sensor 6	0.032× + 0.950	0.998	0.995	5.96	5.46
Sensor 7	0.031× + 0.989	1.000	1.000	4.20	4.10
Sensor 8	0.030× + 1.021	0.999	0.998	3.62	3.13
Sensor 9	0.033× + 0.954	0.998	0.996	7.10	6.67
Sensor 10	0.033× + 1.060	0.999	0.998	11.29	11.00
Sensor 11	0.031× + 0.987	1.000	1.000	4.37	4.31
Sensor 12	0.030× + 1.057	1.000	0.999	5.36	5.15

Abbreviations: MAE = mean absolute error (in %RH); MSE = mean squared error (in %RH); R = correlation coefficient; R^2 = coefficient of determination.

3.3 | Analysis of Microclimatic Conditions

The results demonstrated that the refrigeration system efficiently maintained the air temperature (Ta) in the cold room, with 72% of measurements falling between −1°C and 1°C (Figure 9a,b), in accordance with the thermostatic control settings. However, RH exhibited greater variability (80%–90% RH), remaining below the optimal range of 90%–95% RH recommended for table grapes (Brackmann et al. 2000; Gross et al. 2016). These RH fluctuations were attributed to the on/off cycling of the cooling system and the operation of the sprinklers. From a postharvest perspective, maintaining RH below the recommended range (90%–95%) may intensify water loss in table grapes, leading to stem browning and berry dehydration, which are critical factors affecting market quality (Brackmann et al. 2000; Gross et al. 2016). The results obtained in this study demonstrate that even when temperature is adequately controlled, inadequate humidity management can compromise product preservation, reinforcing that environmental deviations are directly associated with quality deterioration and economic losses in the cold chain (Habib et al. 2024; Canatan et al. 2025). Therefore, continuous monitoring of environmental conditions is essential to

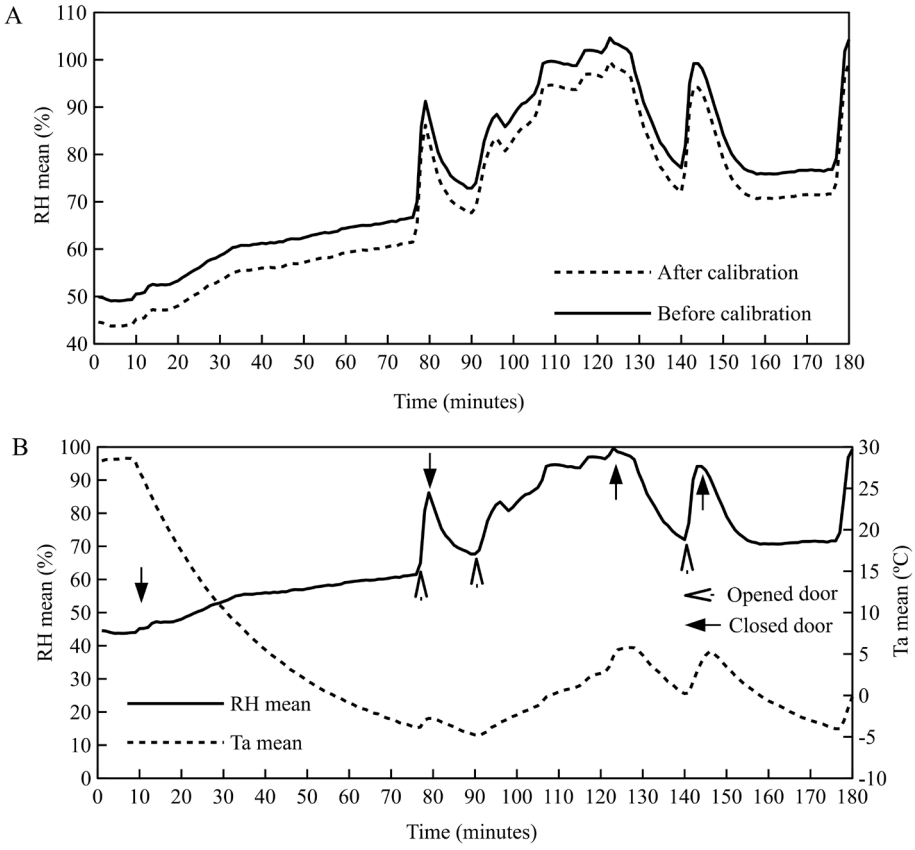

FIGURE 8 | Comparison between RH values obtained using the manufacturer's equation (before calibration) and the calibration curves (after calibration) (A). Temporal variation of Ta and RH in the cold room during UMITEMP evaluation, including a comparison between calibrated and noncalibrated RH values (B).

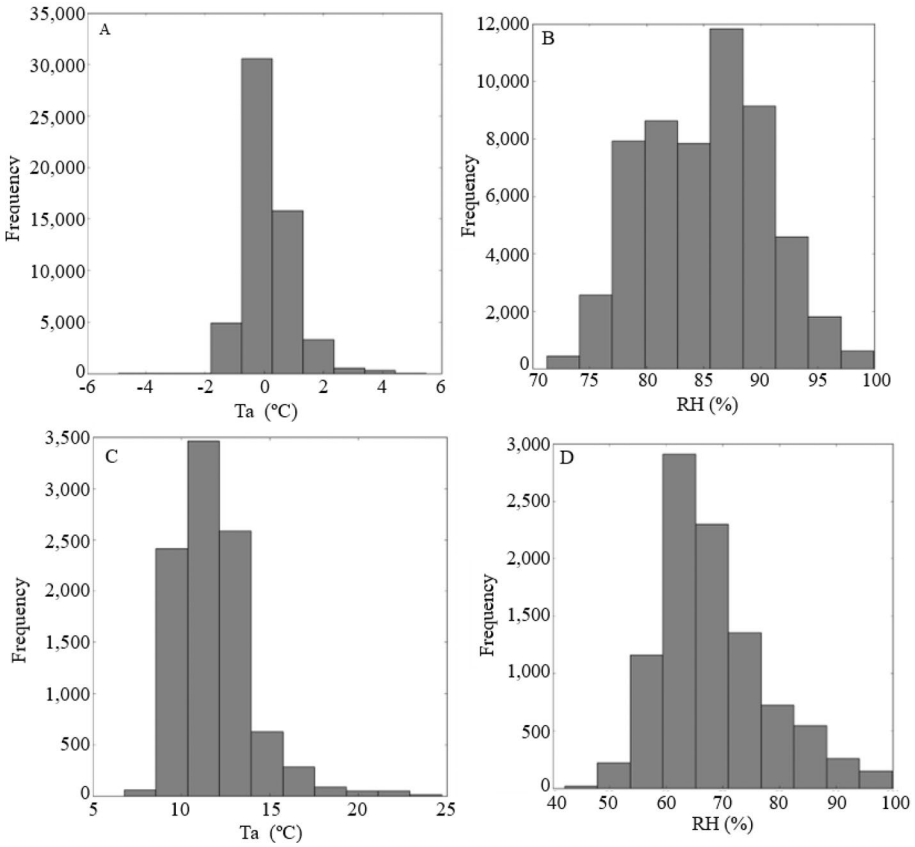

FIGURE 9 | Frequency histograms of Ta (A) and RH (B) in the cold room; Ta (C) and RH (D) in the access corridor.

support decision-making and improve postharvest management (Chaudhuri et al. 2018).

In the access corridor, a distinct thermal profile was observed (Figure 9c,d), with average Ta between 10°C–15°C and RH between 60%–80%, reflecting the influence of the external environment during loading/unloading operations. Extreme values occurred predominantly during peak activity periods, coinciding with intensive pallet handling.

Comparative analysis (Figure 10a,b) revealed low correlation between environments ($R = -0.10$ for Ta; $R = 0.01$ for RH) and negligible covariance (COV = −0.07 for Ta; COV = 0.19 for RH), confirming the effectiveness of thermal insulation. The mean Ta in the cold room (0.4°C ± 0.35°C; mean ± standard deviation) complied with the recommendations for grape storage (−1°C to 0°C) (Crisosto et al. 2001), although peaks of up to 5.4°C were recorded during specific operations.

3.4 | Communication Network Performance

The system implemented compact data packets (10 bytes) exclusively using integer variables, optimizing both transmission and microcontroller processing. Calibration models were integrated through the relational database, ensuring computational efficiency.

Table 2 summarizes the signal quality assessment after 24 h of continuous operation, presenting critical metrics such as total packets sent/received, PLR, and PDR. Results showed that 9 out of the 12 SUs achieved success rates above 97%, while 3 units exhibited losses ranging from 4.25% to 13.10%. According to the classification proposed by (Fan 2015; Melliani and Castillo 2021), UMITEMP qualifies as a soft real-time system, where such packet loss rates are acceptable without compromising system functionality.

The mesh topology proved particularly effective, offering three main advantages: (1) resilience to individual node failures (as evidenced by SU 12, which failed completely without impacting other units), (2) capability for rapid fault diagnosis, and (3) robustness under adverse conditions—as demonstrated by SU 01, which maintained a 99.65% transmission success rate through the insulated chamber walls, and SU 43, which achieved 97.16% success despite being the farthest from the MU.

3.5 | Psychrometric Performance

Psychrometric data (Figure 11) revealed significant differences between the cold chamber and the access corridor throughout the experimental period. Each point in the psychrometric chart represents the mean values of temperature and relative humidity recorded at 1-min intervals during the monitoring period, resulting in a high density of data points that reflect the dynamic behavior of the system in real time. Data from the cold room correspond to the spatially averaged values obtained from all sensor units at each time step, while the corridor data represent measurements from the dedicated sensor installed in that environment. This divergence in air thermodynamic properties indicates minimal heat exchange between the two spaces, demonstrating the effectiveness of the cold chamber's thermal insulation. However, the corridor clearly reflected external environmental influence, with progressive increases in Ta over the days—except on Figure 11e, when it remained stable due to relatively mild external conditions (maximum 26.3°C, minimum 21.6°C). This stable behavior

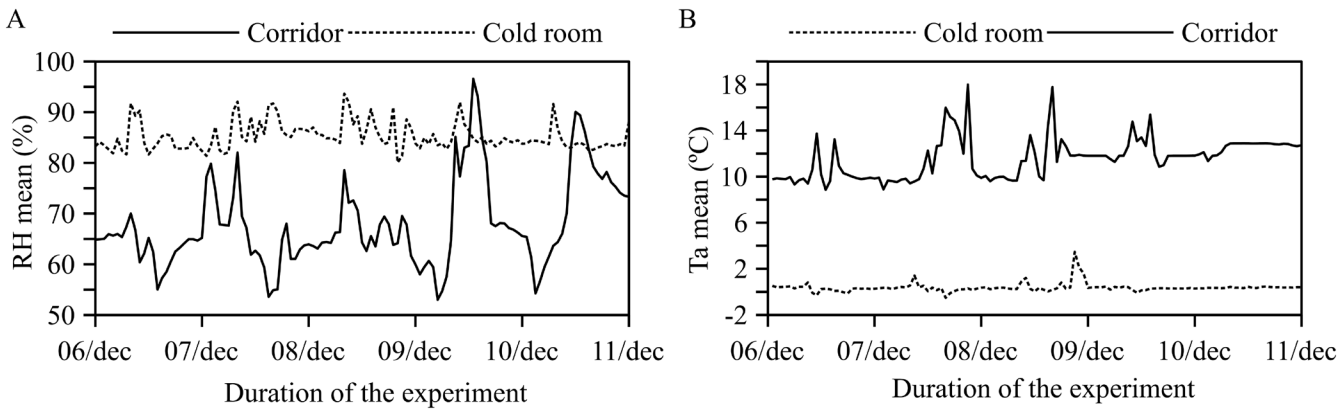

FIGURE 10 | Comparison of average RH (A) and Ta (B) between the corridor and the cold room across different analysis days.

TABLE 2 | Signal quality calculations for the SU.

SU	01	11	12	13	21	22	23	31	32	33	41	42	43
Pd	1422	1365	—	901	1433	1412	906	1322	1426	1418	1336	1422	1408
Pr	1417	1307	—	783	1420	1371	789	1287	1398	1396	1327	1397	1368
PLR	0.35	4.25	—	13.10	0.91	2.90	12.91	2.65	1.96	1.55	0.67	1.76	2.84
PDR	99.65	95.75	—	86.90	99.0	97.10	87.09	97.35	98.04	98.45	99.33	98.24	97.16

Note: total number of packets sent (Pd), total number of packets received (Pr), packet loss rate (PLR), and packet delivery rate (PDR).

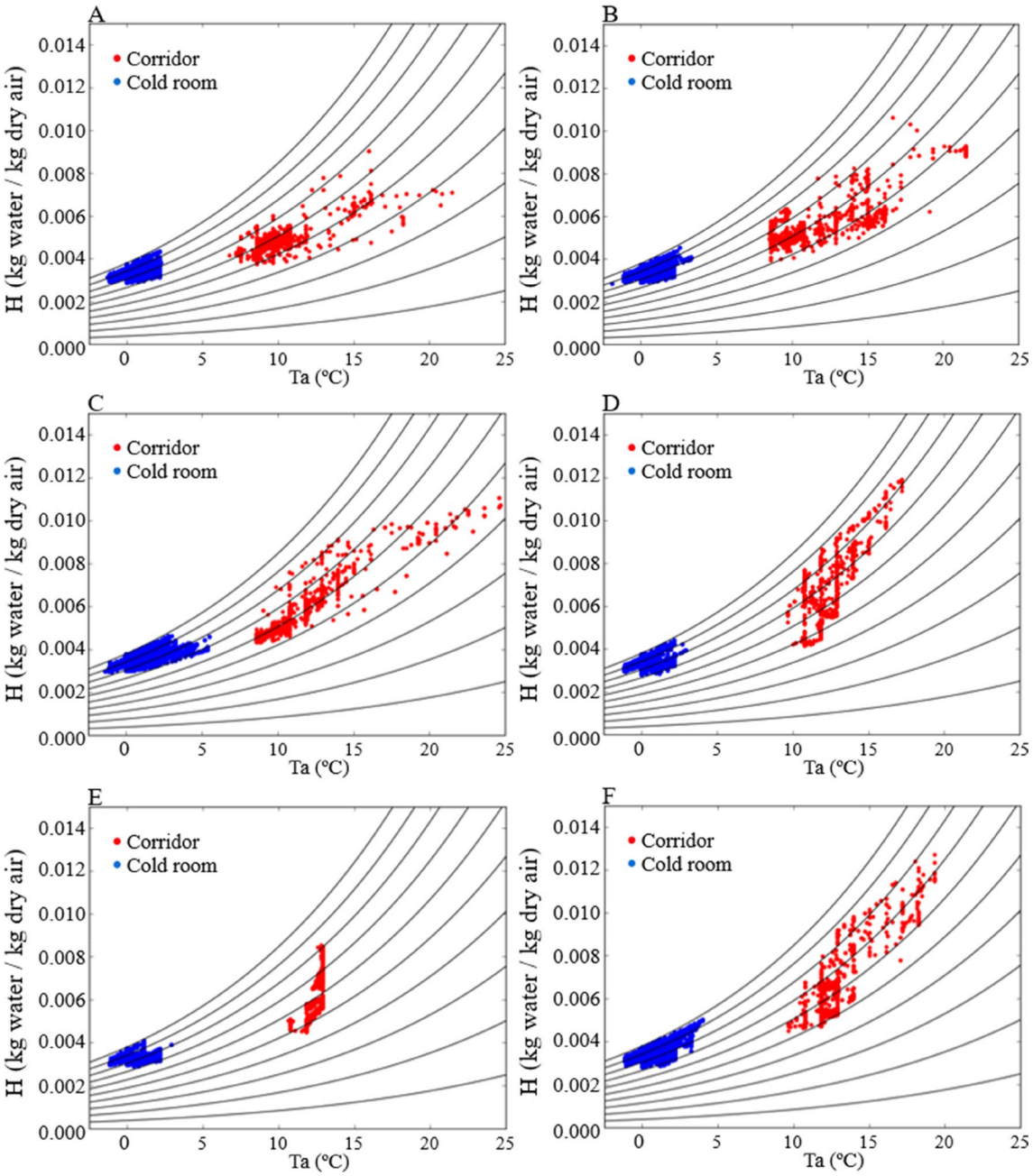

FIGURE 11 | Analysis of air properties in the cold chamber and the corridor during the first (A), second (B), third (C), fourth (D), fifth (E), and sixth (F) day of the experimental period.

on Sunday suggests a strong correlation between thermal variation in the corridor and facility activity levels, which naturally decrease on weekends. Unlike isolated temperature and relative humidity plots, the psychrometric chart allows the simultaneous visualization of the thermodynamic state of the air, enabling the identification of patterns and trajectories that are not evident when variables are analyzed separately, particularly under dynamic operating conditions.

3.6 | Spatial Analysis of Microclimatic Variables

Results revealed distinct spatial patterns in Ta and RH distribution within the cold chamber (Figure 12). The spatial maps presented were generated through postprocessing of the monitored data using geostatistical interpolation methods, allowing a detailed analysis of microclimatic variability within the storage environment. Ta showed both horizontal and vertical variation, with higher values near the entrance and the southern region (mean 0.4°C, range 0.7°C), attributed to corridor influence and solar radiation on the south wall. In contrast, the eastern region displayed lower temperatures due to proximity to the refrigeration system.

Variance analysis (Figure 12b) confirmed lower thermal fluctuation inside the cold chamber (values <1) compared to the corridor (0.22–0.40), though higher than values reported by (Badia-Melis, Ruiz-Garcia, et al. 2015) for nonrefrigerated

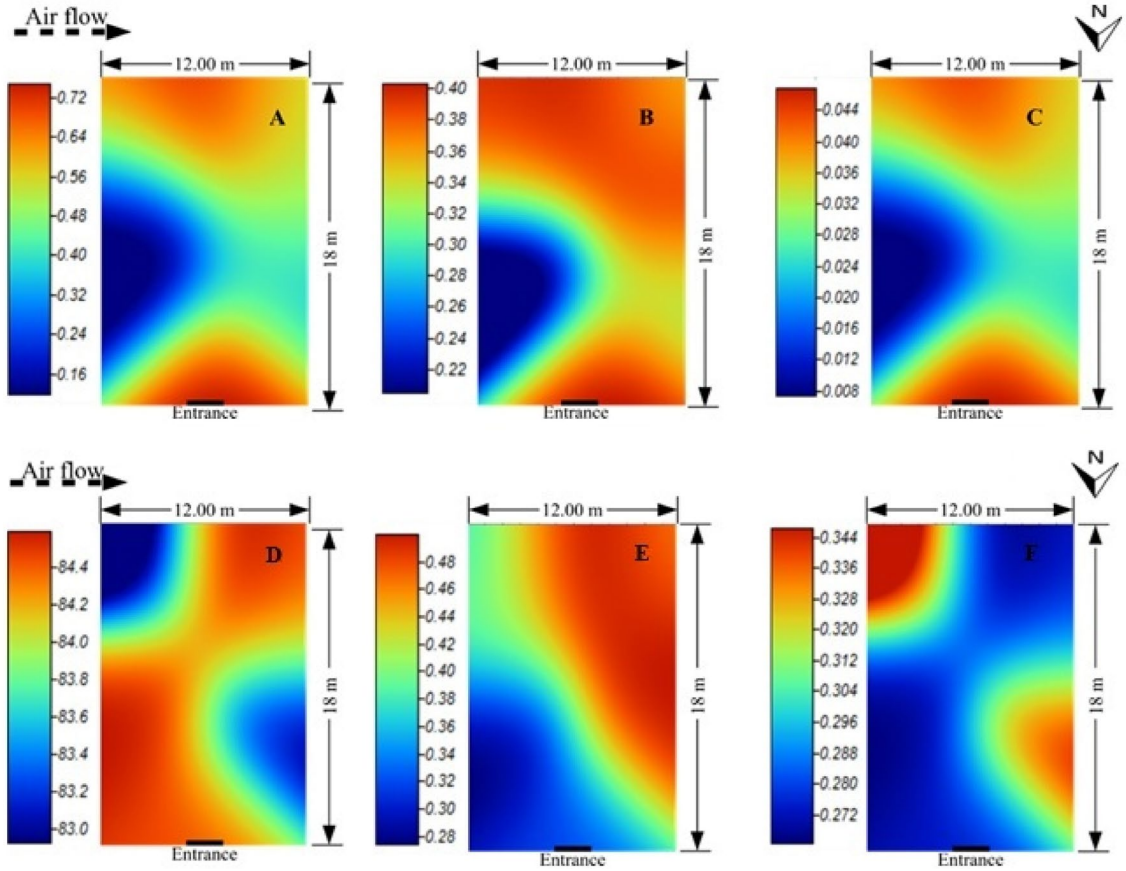

FIGURE 12 | Interpolated Ta maps in the cold room (A); Ta variance in the cold room relative to the corridor (B); normalized Ta difference (C); RH maps in the cold room (D); RH variance in the cold room relative to the corridor (E); and normalized RH difference (F).

corridors (0.005–0.03). Ta remained close to, but slightly above, the ideal value (0°C) for grape storage.

RH exhibited spatial heterogeneity (81%–85%), with lower values in the southeast and northwest regions, correlating with higher Ta areas (Figure 12d). RH variance (Figure 12e) was more pronounced in areas distant from the refrigeration system (0.28–0.48), but always lower than in the corridor. The normalized difference (Figure 12f) indicated RH consistently below the optimal level (90%), with ratios of 0.27–0.34 compared to the corridor.

3.7 | Implications for Storage Management and Monitoring

These findings demonstrate that while thermal insulation proved efficient in most of the cold chamber, vulnerable points were identified, particularly near the entrance and south wall. The analysis also underscores the need to optimize the humidification system, as RH values consistently fell below the 90% recommended for grape storage. Equipment location markedly influenced the thermal gradient, with the refrigeration system creating lower temperature zones in the eastern region. Furthermore, systematic variations were detected, associated with internal airflow patterns. These results highlight specific challenges in precisely controlling environmental conditions for grape storage, particularly in maintaining relative humidity at optimal levels.

The spatial variability identified in this study reinforces the limitation of conventional monitoring approaches based on single-point measurements, which may not capture localized deviations within the storage environment. In the context of table grape storage, these microclimatic differences can result in heterogeneous product quality within the same batch, emphasizing the importance of spatial monitoring as a support tool for decision-making and system optimization (Oliveira et al. 2020; Habib et al. 2024). Therefore, continuous monitoring of environmental conditions is essential to support decision-making and reduce postharvest losses in cold chain systems (Chaudhuri et al. 2018; Canatan et al. 2025).

3.8 | System Advantages and Practical Applications

Compared to conventional monitoring approaches, which are typically based on manual measurements or data loggers with delayed data retrieval, the UMITEMP system provides continuous real-time monitoring combined with spatial analysis. This enables the immediate detection of deviations from optimal storage conditions and supports faster decision-making during critical operations such as loading and unloading (Khumalo et al. 2023). Furthermore, the integration of temporal and spatial data allows for a more comprehensive understanding of microclimatic variability, which is often not captured by traditional offline monitoring systems.

3.9 | Future Perspectives

Although the current system focuses on environmental monitoring, future developments may integrate predictive models to estimate product shelf life based on temperature and humidity dynamics. Furthermore, the inclusion of additional indicators such as mass loss could enhance the system's capability for post-harvest quality assessment.

3.10 | Cost Analysis

An approximate cost analysis indicated that the total implementation cost of the UMITEMP system was R$ 2561.03 in 2018, corresponding to approximately R$ 137.60 per sensor node. After adjusting for inflation to January 2026, the estimated total cost increased to R$ 4631.94, or R$ 248.87 per node. Considering an exchange rate of 1 USD = 5.15 BRL, this corresponds to approximately USD 899.02 for the complete system and USD 48.30 per sensor node.

It is important to note that, despite the inflation-adjusted increase, the cost of electronic components has generally decreased over time due to technological advancements, which may further reduce the current implementation cost. These results highlight the potential of the UMITEMP system as a low-cost alternative for real-time monitoring in cold storage applications.

4 | Conclusion

The UMITEMP system proved to be an effective tool for the continuous monitoring of cold chambers used for table grape storage, demonstrating robustness by maintaining stable wireless sensor network (WSN) data transmission even under adverse conditions imposed by wall insulation, sensor spacing, and microclimatic variations. The results showed that the cold chamber had an average relative humidity (RH) of 85%, ranging from 71% to 100%, which was below the optimal range of 90%–95% recommended for the preservation of seedless grapes. Regarding air temperature (Ta), the mean value of 0.4°C was close to the ideal range (−1°C to 0°C), although extremes between −1.9°C and 5.4°C were recorded during specific operations. Spatial analysis revealed thermal and hygrometric variability inside the chamber, with lower variance compared to the corridor, as well as consistently distinct psychrometric properties between the environments. The corridor was clearly influenced by external conditions, particularly on business days. These findings highlight the system's capability to detect both average conditions and localized fluctuations in the refrigerated environment, providing accurate data for the optimized management of fresh fruit storage, while also indicating the need for adjustments in refrigeration and humidification systems to achieve ideal preservation parameters. Compared to conventional monitoring approaches, the UMITEMP system enables continuous real-time analysis combined with spatial monitoring, allowing the identification of microclimatic variations that are not captured by single-point or offline measurements. This represents a significant advantage for decision-making in cold storage management. Future developments may integrate predictive models and additional quality indicators to further enhance the system's applicability in post-harvest management.

Acknowledgments

The Article Processing Charge for the publication of this research was funded by the Coordenação de Aperfeiçoamento de Pessoal de Nível Superior - Brasil (CAPES) (ROR identifier: 00x0ma614).

Funding

This study was funded by the Fundação de Amparo à Ciência e Tecnologia do Estado da Bahia (FAPESB) (Grant No. 2043/2016). The authors also acknowledge the support of the Coordenação de Aperfeiçoamento de Pessoal de Nível Superior—Brazil (CAPES—Finance Code 001).

Ethics Statement

The authors have nothing to report.

Consent

The authors have nothing to report.

Data Availability Statement

The data that support the findings of this study are available from the corresponding author upon reasonable request.

References

Amorim, M. N., I. B. Miranda, Í. E. A. Santos, et al. 2020. "Plastic Film Bags on the Refrigeration of Table Grapes." *Revista Brasileira de Ciências Agrárias—Brazilian Journal of Agricultural Sciences* 15, no. 4: 1–8. https://doi.org/10.5039/agraria.v15i4a8415.

Amorim, M. N., I. B. Miranda, Í. E. D. A. Santos, D. Lourençoni, and S. H. Turco. 2022. "Fuzzy Modeling for Rapid Cooling of Table Grapes in Different Plastic Film Bags." *Engenharia Agrícola* 42, no. 1: e20200149. https://doi.org/10.1590/1809-4430-eng.agric.v42n1e20200149/2022.

ASAE. 1998. *ASAE D271.2 DEC94: Psychrometric Data*. American Society of Agricultural Engineers.

Badia-Melis, R., U. Mc Carthy, L. Ruiz-Garcia, J. Garcia-Hierro, and J. I. R. Villalba. 2018. "New Trends in Cold Chain Monitoring Applications—A Review." *Food Control* 86: 170–182. https://doi.org/10.1016/j.foodcont.2017.11.022.

Badia-Melis, R., P. Mishra, and L. Ruiz-García. 2015. "Food Traceability: New Trends and Recent Advances. A Review." *Food Control* 57: 393–401. https://doi.org/10.1016/j.foodcont.2015.05.005.

Badia-Melis, R., L. Ruiz-Garcia, J. Garcia-Hierro, and J. Villalba. 2015. "Refrigerated Fruit Storage Monitoring Combining Two Different Wireless Sensing Technologies: RFID and WSN." *Sensors* 15, no. 3: 4781–4795. https://doi.org/10.3390/s150304781.

Brackmann, A., S. M. Mazaro, and A. J. Waclawovsky. 2000. "Armazenamento Refrigerado de Uvas Cvs. Tardia de Caxias e Dona Zilá." *Ciência Rural* 30, no. 4: 581–586. https://doi.org/10.1590/S0103-84782000000400004.

Canatan, M., R. Munoz-Carpena, and Z. Boz. 2025. "Continuous Surface Temperature Monitoring of Refrigerated Fresh Produce Through Visible and Thermal Infrared Sensor Fusion." *Postharvest Biology and Technology* 222: 113354. https://doi.org/10.1016/j.postharvbio.2024.113354.

Chaudhuri, A., I. Dukovska-Popovska, N. Subramanian, H. K. Chan, and R. Bai. 2018. "Decision-Making in Cold Chain Logistics Using Data Analytics: A Literature Review." *International Journal*

of Logistics Management 29, no. 3: 839–861. https://doi.org/10.1108/IJLM-03-2017-0059.

Crisosto, C. H., J. L. Smilanick, and N. Dokoozlian. 2001. "Table Grapes Suffer Water Loss, Stem Browning During Cooling Delays." *California Agriculture* 55, no. 1: 39–42. https://doi.org/10.3733/ca.v055n01p39.

Durner, E. F. 2013. *Principles of Horticultural Physiology*. 1st ed. CABI.

Fabri, A. L. S., A. M. Jordão, A. C. Correia, A. F. Pinto, R. D. D. M. C. Amboni, and M. M. C. Feltes. 2025. "Effect of Storage Temperature on Physicochemical, Physical, Microbiological, and Sensory Characteristics of Table Grapes ('Red Globe'variety')." *Scientia Plena* 21, no. 4: 1–10. https://doi.org/10.14808/sci.plena.2025.041501.

Fan, X. 2015. *Real-Time Embedded Systems: Design Principles and Engineering Practices*. Newnes.

Garrido-López, J., M. Jiménez-Buendía, A. Toledo-Moreo, J. Giménez-Gallego, and R. Torres-Sánchez. 2024. "Monitoring Perishable Commodities Using Cellular IoT: An Intelligent Real-Time Conditions Tracker Design." *Applied Sciences* 14, no. 23: 11050. https://doi.org/10.3390/app142311050.

Greenspan, L. 1977. "Humidity Fixed Points of Binary Saturated Aqueous Solutions." *Journal of Research of the National Bureau of Standards Section A, Physics and Chemistry* 81, no. 1: 89. https://doi.org/10.6028/jres.081A.011.

Gross, K. C., C. Y. Wang, and M. Saltveit. 2016. *The Commercial Storage of Fruits, Vegetables, and Florist and Nursery Stocks (No. 348552)*. United States Department of Agriculture. https://doi.org/10.22004/ag.econ.348552.

Habib, M., B. Lyons, and C. Renando. 2024. "Adoption Challenges of Environmental Monitoring Practices: Case Study of Temperature Data Loggers in Selected Australian Vegetable Supply Chains." *Applied Water Science* 14, no. 12: 260. https://doi.org/10.1007/s13201-024-02300-5.

Ibrahim, A. M., and R. H. A. Nasser. 2015. "Comparison Between Inverse Distance Weighted (IDW) and Kriging." *International of Science and Research* 6, no. 11: 249–254. https://doi.org/10.21275/ART20177562.

Kamilaris, A., A. Kartakoullis, and F. X. Prenafeta-Boldú. 2017. "A Review on the Practice of Big Data Analysis in Agriculture." *Computers and Electronics in Agriculture* 143: 23–37. https://doi.org/10.1016/j.compag.2017.09.037.

Karimi, N., A. Arabhosseini, M. Karimi, and M. H. Kianmehr. 2018. "Web-Based Monitoring System Using Wireless Sensor Networks for Traditional Vineyards and Grape Drying Buildings." *Computers and Electronics in Agriculture* 144: 269–283. https://doi.org/10.1016/j.compag.2017.12.018.

Khumalo, G., L. L. Goedhals-Gerber, P. Cronje, and T. Berry. 2023. "Product Visibility in the South African Citrus Cold Chain: Examining the Efficacy of Temperature Loggers." *Heliyon* 9, no. 1: e12732. https://doi.org/10.1016/j.heliyon.2022.e12732.

Korotcenkov, G. 2018. *Handbook of Humidity Measurement, Volume 1: Spectroscopic Methods of Humidity Measurement*. 1st ed. CRC Press.

Kumari, L., K. Narsaiah, M. K. Grewal, and R. K. Anurag. 2015. "Application of RFID in Agri-Food Sector." *Trends in Food Science & Technology* 43, no. 2: 144–161. https://doi.org/10.1016/j.tifs.2015.02.005.

Lazzarotto, J. J., and J. C. Fioravanço. 2012. "Comércio Exterior Mundial e Brasileiro de uva de Mesa: Análise de Indicadores de Competitividade, Tendências e Sazonalidades." https://www.sidalc.net/search/Record/dig-infoteca-e-doc-956550/Description.

Mayer, S., J. Reuder, and J. Schween. 2005. "Calibration of Capacitive Humidity Sensors for Atmospheric Sounding by Remotely Piloted Vehicles."

Melliani, S., and O. Castillo. 2021. *Recent Advances in Intuitionistic Fuzzy Logic Systems and Mathematics*. 1st ed. Springer. https://doi.org/10.1007/978-3-030-53929-0.

Miranda, I. B., Í. E. D. A. Santos, M. D. N. Amorim, S. H. Turco, and A. C. D. S. Lins. 2025. "Climatized Packing House With Evaporative Coolers-Part 2: Geostatistical Mapping." *Revista Brasileira de Engenharia Agricola e Ambiental* 29, no. 6: e281082. https://doi.org/10.1590/1807-1929/agriambi.v29n6e281082.

Mohammed, M., K. Riad, and N. Alqahtani. 2022. "Design of a Smart IoT-Based Control System for Remotely Managing Cold Storage Facilities." *Sensors* 22, no. 13: 4680. https://doi.org/10.3390/s22134680.

Nair, N. R., P. W. McCarthy, A. I. Heusch, and R. Patz. 2015. *Testing the Reliability of Humidity Sensors Through Prolonged Measurements Traceable to Calibration Standards. In 17th International Congress of Metrology*, 15002. EDP Sciences.

Oliveira, C. C. M. D., D. R. B. D. Oliveira, and V. Silveira. 2020. "Variability in the Shelf Life of Table Grapes From Same Batch When Exposed Under Different Ambient Air Conditions." *Food Science and Technology* 41, no. suppl 1: 290–300. https://doi.org/10.1590/fst.14220.

Pereira, E., W. A. Spagnol, and V. Silveira Junior. 2018. "Water Loss in Table Grapes: Model Development and Validation Under Dynamic Storage Conditions." *Food Science and Technology* 38: 473–479. https://doi.org/10.1590/1678-457x.08817.

Rivero, R. A. G., L. E. M. Hernández, O. Schalm, et al. 2023. "A Low-Cost Calibration Method for Temperature, Relative Humidity, and Carbon Dioxide Sensors Used in Air Quality Monitoring Systems." *Atmosphere* 14, no. 2: 191. https://doi.org/10.3390/atmos14020191.

Santos, Í. E. D. A., W. M. Okita, D. Lourençoni, et al. 2025. "Neuro-Fuzzy Modeling of Pulp Temperature in Rapid Cooling Chamber." *Journal of Food Science and Technology* 62, no. 6: 1110–1115. https://doi.org/10.1007/s13197-024-06109-7.

Webster, J. G., and H. Eren. 2018. *Measurement, Instrumentation, and Sensors Handbook: Two-Volume Set*. 2nd ed. CRC Press.

Whitaker, J. H., and E. R. Dawson. 2025. "Cold Chain Logistics Thermal Reliability: Modeling Temperature Excursions, Sensor Uncertainty, and Time-To-Intervention for Perishable Supply Chains." *Techne: Journal of Engineering, Technology and Industrial Applications* 1, no. 2: 36–49.

World Meteorological Organization. 2008. *Guide to Instruments and Methods of Observation (WMO-No. 8)*. WMO.

Zhang, Q., S. Huang, L. Feng, J. Zhang, and T. Ren. 2024. "Design of a Temperature and Humidity Calibration Device for Cold Chain Warehousing and Transportation." In *Proceedings of the Ninth International Symposium on Sensors, Mechatronics, and Automation System (ISSMAS 2023)* (Vol. 12981, 550–557). SPIE. https://doi.org/10.1117/12.3015006.